Scalable Computing: Practice and Experience, ISSN 1895-1767, http://www.scpe.org
© 2024 SCPE. Volume 25, Issues 5, pp. 4246–4254, DOI 10.12694/scpe.v25i5.3192

DIMENSION EXTRACTION OF REMOTE SENSING IMAGES IN TOPOGRAPHIC SURVEYING BASED ON NONLINEAR FEATURE ALGORITHM

YANI WANG*, YINPENG ZHOU†, AND BO WANG ‡

Abstract. In order to solve the problem of inaccurate image feature extraction caused by traditional extraction methods, this paper proposes a remote sensing image size extraction method based on nonlinear multi feature fusion for topographic maps. In this paper, SVM and DS evidence theory are combined to extract image features and classify pre processed remote sensing images. Based on the classification results, basic probability distributions are constructed, and a DS fusion algorithm using matrix analysis is introduced to simplify the complexity of decision level fusion algorithms; We use a multi feature fusion algorithm based on feature proximity, using the proximity vector formed by the attraction between the feature vector and the original graphics pattern as the fusion feature to complete the extraction of remote sensing image features. The simulation results show that after using this method, its soft threshold classifier outputs 0.9865, 0.9965, 0.7852, 0.9921, 0.9847, 0.6879, -0.5898, -0.5678, -0.6897, -0.4785. The algorithm in this paper can distinguish the shape features of terrain images well, and can extract the features of terrain images more accurately, which has strong feasibility.

Key words: Image feature extraction, Multi-feature fusion, Matrix analysis, Feature proximity, Feature vector

1. Introduction and examples. Remote sensing technology has become a comprehensive technology integrating multiple fields after decades of development since the 1960s [1]. Remote sensing technology refers to the observation of ground objects through some devices, obtaining relevant data, but not directly contacting the observation objects, and extracting and excavating the information from the obtained data. Different sensors have different spectral resolution. Generally, the imaging of remote sensing technology can be divided into the following categories according to the different resolution:

① Multispectral remote sensing image: the spectral resolution is within the range of 10-1λ, and the multispectral image only contains 3-4 spectral bands, which contains less information;

② Hyperspectral remote sensing image: the spectral resolution is within 10-2λ, often with tens to hundreds of bands, and contains rich information. This paper takes hyperspectral image as the main research object;

③ Ultra-spectral remote sensing image: the spectral resolution is within the range of 10-3λ, and this paper does not involve ultra-hyperspectral image [2].

Hyperspectral remote sensing technology is one of the latest achievements of remote sensing technology. It scans objects and obtains relevant information through a series of narrow electromagnetic wave bands. The sensor forms a spectral image through hyperspectral remote sensing technology. The image contains continuous spectral information. Researchers can use this information to find some hidden material information, which is one of the advantages of hyperspectral remote sensing. Therefore, hyperspectral sensor imaging is a powerful assistant for researchers to identify substances in detail and accurately estimate the abundance of substances [3].

With the vigorous development of hyperspectral remote sensing technology in hardware, it is gradually recognized and accepted by more people, and the application field of remote sensing technology has been greatly expanded. But the puzzle behind the rapid development of remote sensing hardware technology is that a large number of remote sensing data are just cold numbers, which have not been fully utilized and mined, let alone used to serve mankind.

*Xi'an University, Shaanxi, Xi'an, 710065, China (YaniWang53@126.com)
†Institute of Surveying and Mapping Guizhou Geology and Mineral Exploration Bureau (Corresponding author, YinpengZhou7@163.com)
‡Shaanxi Geomatics Center, Ministry of Natural Resources Xi'an, China (BoWang28@126.com)

The data collected by hyperspectral remote sensing technology contains a lot of information, through which the spectral characteristics of the observed object can be closely linked with the spatial geographic information, and many potential characteristics of substances can be easily mined by analyzing hyperspectral data, which are important reasons why hyperspectral images are favored by more and more remote sensing experts. The hyperspectral remote sensing technology not only obtains the spectral characteristics of the ground object, but also preserves the relationship between the observed object and other surrounding ground objects. The resulting images contain rich information, which provides a strong support for us to use and analyze data.

2. Literature review. Buildings are an important component of urban areas. The technology of automatic extraction of buildings by computer is widely used in the fields of urban large-scale topographic map drawing, urban planning, urban geographic information system construction and military reconnaissance. Driven by these applications, many automatic building extraction methods have emerged. In recent years, automatic building extraction from remote sensing images has become a hot spot, attracting many scholars to discuss and study, and put forward many detection models and methods [4]. After summary, we can classify it into two kinds of methods: traditional building detection algorithm and building detection algorithm based on machine learning. Traditional building detection algorithms focus on describing the underlying features of buildings, such as building detection based on gray scale, contour, texture and other features or a simple combination of several underlying features, and building detection algorithms that add laser point clouds, DEM and other data sources [5]. Building detection algorithm based on gray level: This kind of method is mainly to analyze the gray level distribution in the image. Due to the different reflectivity of the building roof and other ground objects to the sunlight, there will be gray level differences, so the building will be extracted from the image using the region segmentation algorithm; Because most buildings have shadows, the gray contrast between the shadows around the buildings and the background is used to detect the existence of buildings.

Therefore, Li, X proposed a multivariate fusion voting network (MFFVoteNet) framework to improve the performance of 3D object detection in non-uniform and high-impact environments. Our method uses a point cloud and a synchronized RGB image as input to enable object detection in 3D space [6]. Shankar, K Review of WSI review process based on machine learning. First, the development status of WSI and CAD methods is presented. Second, we discuss WSI data reporting, segmentation, classification, and metrics for testing activities [7]. Wang, Z proposed a novel fusion model based on meta-heuristics for diagnosing COVID-19 using chest radiographs. The model includes various preplanning, extraction procedures and categories. Initially, Wiener filter (WF) technology was used for image processing [8].

This paper proposes a feature extraction method of remote sensing image based on SVM and multi-feature fusion. The simulation results show that the accuracy and speed of pixel extraction of the method proposed in this paper are much higher than those of traditional methods in the process of image extraction, which can be widely used and has strong feasibility.

3. Research methods.

3.1. Remote sensing image feature extraction principle. This is because traditional remote image feature extraction has many different parameters and is capable of extracting pixel features and recovering them in time and frequency. Therefore, we can use this model to analyze and extract the local features of remote sensing images during time and frequency changes, which is increasingly used after the remote sensing image is completed [9]. Traditional remote sensing image post-processing involves extracting the main features of multi-pixel lines from the original image by reconstructing and analyzing frequency pixels during two-dimensional frequency transfer to the area.

3.1.1. Pretreatment before feature extraction of remote sensing image.

(1) Pixel domain subband analysis of remote sensing image. For $P_0, (\Delta_s, s \geqslant 0)$ in the post-processing of captured image pixels. Restore the image pixels $(P_0 f, \Delta_1 f, \Delta_2 f, ...)$ of different sub-bands for the pixel range f, and the sub-band $\Delta_s f$ of multi-dimensional space contains the main features with the pixel space of 2^{-2s}.

(2) Pixel smooth segmentation of remote sensing image. In the process of restoring the remote sensing image pixels, set the set of $\omega_Q(x_1, x_2)$, and calculate the corresponding function ω_Q of a parameter of the restored image pixel within a two-dimensional space range of 2^{-2s} to obtain the set of Q similar results, as

follows 3.1:

$$Q = [k_1/2^s, (k_1+1)/2^s] \times [k_2/2^s, (k_2+1)/2^s] \tag{3.1}$$

Run such calculations for image pixel restoration Q of a specific algorithm. Assuming that all image post-processing $Q = Q(s, k_1, k_2)$, and the s similarity segmentation parameters k_1 and k_2 change, as shown in the following formula 3.2:

$$\Delta_s f \to (\omega_Q \Delta_s f)_{Q \in Q_2} \tag{3.2}$$

(3) Normalization of pixels. For a second order square, normalize $(T_Q f)(x_1, x_2) = 2^s f(2^s x_1 - k_1, 2^s x_2 - k_2)$ to calculate pixel f, and the result of Q parameter function calculated by 3.2 is $[0, 1]^2$,as shown in the following formula 3.3:

$$g_Q = (T_Q)^{-1}(\omega_Q \Delta_s f), Q \in Q_s \tag{3.3}$$

The normalization operation of pixels can collect the post-processed pixels and lay the foundation for image fusion extraction.

3.1.2. Extraction and reconstruction of remote sensing image features.

1) Remote sensing image feature straight ridge synthesis. After analyzing the straight ridge extracted from remote sensing image fusion, any calculation parameter is newly created from the orthogonal image pixel set, as shown in the following formula 3.4:

$$g_Q = \sum_{\lambda} \alpha(\lambda, Q) \rho_\lambda \tag{3.4}$$

2) Feature normalization of remote sensing image. The calculation in formula 3.4 can put any pixel into a suitable spatial position, as shown in formula 3.5:

$$h_Q = (T_Q) g_Q, Q \in Q_S \tag{3.5}$$

3) Feature fusion and smooth synthesis of remote sensing image. The result of formula 3.5 can be used as the inverse operation of image feature fusion boundary, as shown in formula 3.6:

$$\Delta_S f = \sum_{Q \in Q_S} \omega_Q - h_Q \tag{3.6}$$

4) Time frequency subband reconstruction. Incorporate formula 3.6, and use image pixel reconstruction formula to reconstruct and synthesize time and frequency, as shown in formula 3.7:

$$f = p_0(p_0 f) + \sum_{s>0} \Delta_s(\Delta_s f) \tag{3.7}$$

3.2. Image feature extraction method based on SVM and multi-feature fusion. Hard interval maximization support vector machine, also known as linear support vector machine, is the most primitive and simplest form of support vector machine [10]. As the basis of support vector machine theory (hereinafter referred to as SVM for short), it mainly aims at the problem of linearly separable dichotomous problems, as shown in Figure 3.1.

First, we combine SVM and DS evidence theory, extract three types of features of image shape, texture and fractal dimension after preprocessing the remote sensing image, and construct basic probability assignment with the SVM classification results of three types of nonlinear single features as independent evidence, and introduce DS fusion algorithm based on matrix analysis to simplify the complexity of decision level fusion algorithm [11]. Multi-feature fusion algorithm is introduced to calculate the spatial approximation of the original graphic pattern and feature vector, and the approximation is used as the fusion feature to complete the extraction of image features.

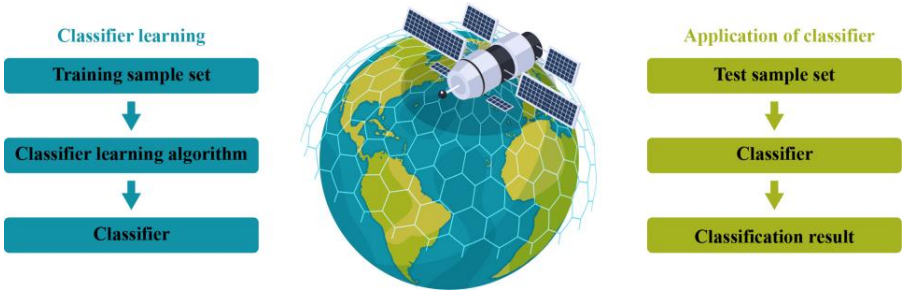

Fig. 3.1: Learning and application of classifier

3.2.1. Theoretical evidence of SVM . The main theoretical basis of the SVM calculation method is the certainty of the specific position of pixels in the dimension space of remote sensing image and the balance interval between each other during the post-processing of image capture. The spatial classification of any number of remote sensing image pixels in the shape, texture and fractal dimension of the image is carried out by using the formula of SVM classification and archiving. The specific method of discrimination is as follows 3.8:

$$f(x) = sgn(\sum_{x_i \in S_V}^{n} a_i y_i k(x_i, x) + b) \tag{3.8}$$

In the above formula, a_i is the Lagrange multiplier, S_V is the support vector, $k(x_i, x)$ is the kernel function, x_i and y_i are the basic support vector bases of the two calculation methods' functions, and b is the parameters determined according to the specific image pixel functions[12].

From the above formula, it can be seen that k(k-1)/2 SVM classification calculation methods are used to restore remote sensing image pixels. In the process of classifying image pixels, the computer defaults to counting once for each calculation, and sends data to all sets. Finally, the most counted image pixels are classified into a class of image pixel sets to build the theoretical evidence of SVM.

3.2.2. DS evidence theory. The basic principle of DS evidence theory is as follows: DS evidence theory fuses the trust functions corresponding to two or more evidence bodies and transforms them into a new function. The implementation process of DS evidence theory is described as follows:

Let Θ be the discriminant framework, define the function $m : 2^{\Theta} \to [0, 1]$ to satisfy the condition $M(\Phi) = 0$ (Φ is empty set), $\sum m(A) = 1(A \in 2^{\Theta})$, and construct $m(A)$ according to the three characteristics of image shape, texture and fractal dimension, which is the fundamental probability assignment (BPA) on the framework Θ. $m(A)$ is the accurate level of trust in proposition A, and $M(\Phi)$ is the uncertainty of evidence. Assuming that $m_1, m_2, ..., m_n$ is BPA to distinguish different evidences on frame Θ, $m = m_1 \bigoplus m_2 \bigoplus ... \bigoplus m_n$ can be converted into the following formula 3.9 and 3.10 according to $\sum m(A) = 1(A \in 2^{\Theta})$:

$$m(A) = \sum_{A_1 \cap A_2 \cap ... \cap A_n = A} (\prod_{1 \leqslant i \leqslant n} m_i(m_i(A)/(1-k)) \tag{3.9}$$

$$k = \sum_{A_1 \cap A_2 \cap ... \cap A_n = A} (\prod_{1 \leqslant i \leqslant n} m_i(m_i(A)) \tag{3.10}$$

In the above formula, k is the uncertainty factor of credentials.

3.2.3. DS-synthesis algorithm with matrix analysis. This paper proposes a DS-synthesis algorithm based on matrix analysis to fuse the features of remote sensing images. In view of the situation of identifying

a target with n-type image features at the same time, the mutually independent fundamental trustable distribution values m_{ij} and uncertainty probability θ_{ij} of n-type features given to m image target categories can be described as the following formula 3.11:

$$M = \begin{bmatrix} m_{11} & m_{12} & \cdots & m_{1m} & \theta_1 \\ m_{21} & m_{22} & \cdots & m_{2m} & \theta_2 \\ \cdots & \cdots & \cdots & \cdots & \cdots \\ m_{n1} & m_{n2} & \cdots & m_{nm} & \theta_n \end{bmatrix} \tag{3.11}$$

Because the sum of the mutually independent fundamental trustable distribution value m_{ij} and uncertainty probability θ_{ij} given to the target category of m images by the same image characteristics should be 1, therefore, the sum of the elements in each row of the matrix should meet the normalization condition, as shown in the following formula 3.12:

$$m_{i1} + m_{i2} + \cdots + m_{im}\theta_i = 1 \tag{3.12}$$

Under the condition of normalization, a new matrix R with $(m+1)\times(m+1)$ is obtained by multiplying the transposition of one row of the matrix with another row, and the DS synthesis of matrix analysis is realized[13]. The following formula 3.13:

$$R = M_i^T M_j \begin{bmatrix} m_{i1}m_{j1} & m_{i2}m_{j2} & \cdots & m_{i1}m_{jm} & m_{i1}\theta_j \\ m_{i2}m_{j1} & m_{i2}m_{j2} & \cdots & m_{i2}m_{jm} & m_{i2}\theta_j \\ \cdots & \cdots & \cdots & \cdots & \cdots \\ m_{im}m_{j1} & m_{im}m_{j2} & \cdots & m_{im}m_{jm} & m_{im}\theta_j \\ \theta_i m_{j1} & \theta_i m_{j2} & \cdots & \theta_i m_{jm} & \theta_i m_j \end{bmatrix} \tag{3.13}$$

where the uncertainty factor k is the sum of the non-diagonal elements of the first $m \times n$ sub-matrices in the matrix, that is, the following formula 3.14:

$$k = \sum_{p \neq q} R_{pq}(p, q = 1, 2, ..., m) \tag{3.14}$$

Fusion of matrix analysis and image features under the DS evidence theory m algorithm: this algorithm completes the matrix multiplication calculation of m+1-dimensional column vector and m+1-dimensional row vector in each implementation process. The time required to obtain the fusion result is $T((m+1)^2)$, and the time required to obtain the fusion result is $T((m+1)^2 n)$, which is approximately linear with the number of characteristic types n[14].

3.2.4. Proximity of remote sensing image features. The feature extraction of remote sensing images is based on the fusion results of image features calculated by the -synthesis algorithm of matrix analysis. The feature space corresponding to the image to be classified is regarded as the core point of the type. The core point is attractive to all feature points in the feature space of the shape, texture and fractal dimension of the remote sensing image. The closer the feature point is to the core point, the stronger the attraction. The attraction of the core point of each image feature type is only effective in a certain spatial range.

Definition 1. In the feature space of the n-dimensional remote sensing image, the attraction between the core point x_i and the feature point x_j is defined as the following formula 3.15:

$$G_{ij} = e^{-d_{ij}^2/2\sigma^2} \tag{3.15}$$

where $d_{ij}^2 = x_i - x_j$ is the Euclidean distance of the two remote sensing image feature vectors, and σ is the parameter that controls the influence range of the core point of the image feature parameters. The core points of remote sensing image feature parameters are attractive to feature points, and the core points also attract each other[15]. The attractiveness index between the core points constitutes the proximity matrix G.

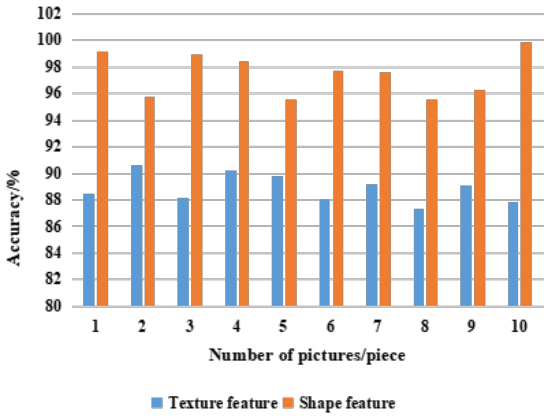

Fig. 4.1: Classification accuracy of target samples detected by SVM classification

Definition 2. Suppose there are m samples in the n-dimensional feature space, and the proximity matrix G is defined as the following formula 3.16:

$$G = \begin{bmatrix} G_{11} & G_{12} & \cdots & G_{1m} \\ G_{21} & G_{22} & \cdots & G_{2m} \\ \cdots & \cdots & \cdots & \cdots \\ G_{m1} & G_{m2} & \cdots & G_{mm} \end{bmatrix} \tag{3.16}$$

Line i in G represents the attraction between the prototype model of image feature type and other prototype models of remote sensing image feature type, which qualitatively reflects the statistical relationship between all types of data and prototype models. G is a symmetric matrix whose diagonal elements are 1. For any remote sensing image sample feature y, it is necessary to calculate the attraction between y and the prototype model of each remote sensing image type. The feature proximity vector g of the image sample is formed by these attractive indicators, which represents the fusion feature of the remote sensing image sample y. The proximity vector is composed of the attraction between the feature vector and the primitive graphic pattern, and the Euclidean distance of the row vector in g and G is compared. If the distance between g and G is close, the feature type of the image sample can be determined to complete the feature extraction of the remote sensing image[16].

4. Result analysis. In order to prove the usefulness of the method in this paper, it is necessary to carry out experimental proof. In the experiment, 300 remote sensing images are used as target samples for testing. Among them, 150 remote sensing images are all kinds of terrain with different angles, and 150 images are other targets. 90 representative remote sensing images of grassland, road, lake and 60 other target images were selected for training after feature acquisition[17].

4.1. Image feature vector classification detection. This paper lists 10 images that are sent into the classifier to implement classification accuracy after the method changes in this paper, as shown in Figure 4.1.

After using this method, the output of its soft threshold classifier is as follows: 0.9865, 0.9965, 0.7852, 0.9921, 0.9847, 0.6879, - 0.5898, - 0.5678, - 0.6987, - 0.4785. The results show that the algorithm in this paper has a good discrimination of the shape features of the terrain image, and can extract the features of the terrain image more accurately.

The remote sensing image in the randomly collected target sample passes through the feature acquisition channel, and is brought into the optimal classification function to check whether it is a terrain image. In the case of no noise, the error of the extraction results of the three types of image features is around 0.0500[18]. Considering that the noise will affect the detection results, 0 2 Gaussian white noise is added to the original image, and its shape, texture and fractal dimension consequences are shown in Figure 4.2 to Figure 4.4.

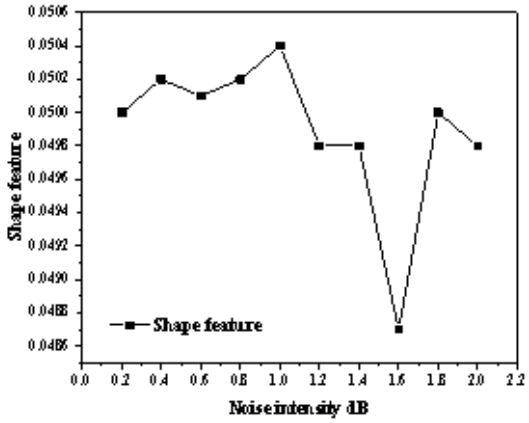

Fig. 4.2: Shape feature error after adding noise

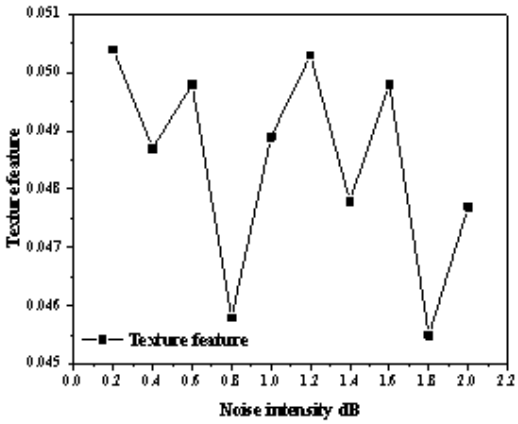

Fig. 4.3: Texture feature error after adding noise

It can be seen from Figure 4.2 to Figure 4.4 that the error range of the result after adding noise is basically the same as that of the noise-free case when the three types of feature vectors extracted by the algorithm in this paper are used for classification detection, with good noise resistance and robustness.

4.2. Comparison results with traditional methods. In order to verify the superiority of this method, we use this method and the traditional method to compare the images of the same sample set, and the results are shown in Figure 4.5 [19].

It can be seen from Figure 4.5 that the accuracy of feature extraction of the method in this paper is significantly higher than that of the traditional method when tested with the method in this paper and the traditional method respectively[20].

5. Conclusion. At present, in the post-processing of image capture, the restoration of image pixels is the key in the whole image processing process, and in the pixel restoration process, the key problem is feature extraction. In addition, the feature extraction of image pixels also has a significant impact on the subsequent

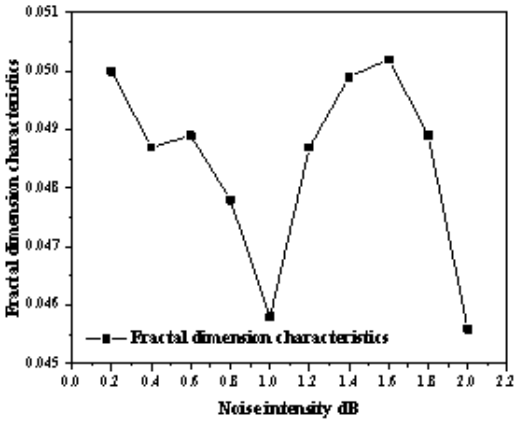

Fig. 4.4: Fractal dimension characteristic error after adding noise

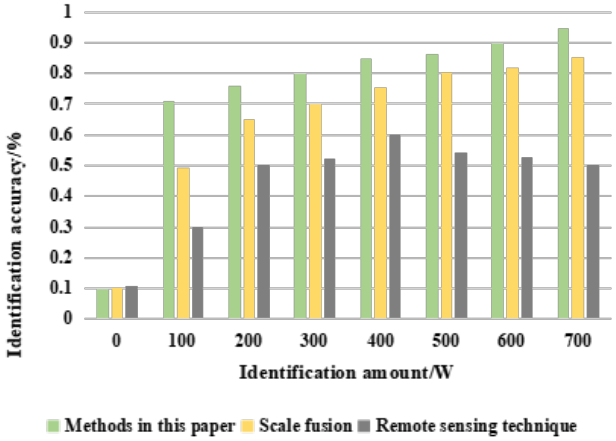

Fig. 4.5: Comparison of image feature extraction accuracy between traditional method and this method

work of image restoration and image calculation. This paper proposes a feature extraction method of remote sensing image based on SVM and multi-feature fusion. The simulation results show that the speed and accuracy of feature extraction of the proposed method are significantly improved compared with traditional methods, which verifies the feasibility of the proposed method. The method of extracting dimensions from remote sensing images of terrain surveying based on nonlinear multi feature fusion has many future research possibilities and areas for improvement. Here are some directions that can be further explored and improved:

1. Feature selection and extraction algorithm: more advanced Feature selection and extraction algorithm can be studied to better capture relevant information in remote sensing image of topographic mapping. For example, automatic feature learning techniques in deep learning models can be explored, as well as specific feature extraction methods that are more suitable for terrain surveying.
2. Data augmentation and incremental learning: Remote sensing images of terrain surveying may have different variation patterns and uncertainties. Therefore, data augmentation techniques can be studied to increase the diversity of training data through operations such as synthesis, rotation, and scaling,

thereby improving the robustness and generalization ability of the model. In addition, introducing incremental learning methods can achieve rapid adaptation to new data and model updates to cope with constantly changing terrain conditions.

REFERENCES

[1] Hosgurmath, S., Mallappa, V. V., Patil, N. B., & Petli, V. (2022). A face recognition system using convolutional feature extraction with linear collaborative discriminant regression classification. International Journal of Electrical and Computer Engineering (IJECE), 12(2), 1468-1476.

[2] Seçkin, A. Ç., & Seckin, M. (2022). Detection of fabric defects with intertwined frame vector feature extraction. Alexandria Engineering Journal, 61(4), 2887-2898.

[3] Vyas, R., Kanumuri, T., Sheoran, G., & Dubey, P. (2022). Accurate feature extraction for multimodal biometrics combining iris and palmprint. Journal of Ambient Intelligence and Humanized Computing, 13(12), 5581-5589.

[4] Sun, L., Zhao, G., Zheng, Y., & Wu, Z. (2022). Spectral–spatial feature tokenization transformer for hyperspectral image classification. IEEE Transactions on Geoscience and Remote Sensing, 60, 1-14.

[5] Ding, Y., Zhang, Z., Zhao, X., Hong, D., Cai, W., Yu, C., ... & Cai, W. (2022). Multi-feature fusion: graph neural network and CNN combining for hyperspectral image classification. Neurocomputing, 501, 246-257.

[6] Li, X., Li, C., Rahaman, M. M., Sun, H., Li, X., Wu, J., ... & Grzegorzek, M. (2022). A comprehensive review of computer-aided whole-slide image analysis: from datasets to feature extraction, segmentation, classification and detection approaches. Artificial Intelligence Review, 55(6), 4809-4878.

[7] Shankar, K., Perumal, E., Tiwari, P., Shorfuzzaman, M., & Gupta, D. (2022). Deep learning and evolutionary intelligence with fusion-based feature extraction for detection of COVID-19 from chest X-ray images. Multimedia Systems, 28(4), 1175-1187.

[8] Wang, Z., Xie, Q., Wei, M., Long, K., & Wang, J. (2022). Multi-feature fusion votenet for 3d object detection. ACM Transactions on Multimedia Computing, Communications, and Applications (TOMM), 18(1), 1-17.

[9] Zhao, L., & Zhu, Q. (2022). Image denoising algorithm of social network based on multifeature fusion. Journal of Intelligent Systems, 31(1), 310-320.

[10] Zhang, Z., & Wang, M. (2022). Multi-feature fusion partitioned local binary pattern method for finger vein recognition. Signal, Image and Video Processing, 16(4), 1091-1099.

[11] Guo, L. (2022). SAR image classification based on multi-feature fusion decision convolutional neural network. IET Image Processing, 16(1), 1-10.

[12] Huang, X., Liu, Y., Wang, Y., & Wang, X. (2022). Feature extraction of search product based on multi-feature fusion-oriented to Chinese online reviews. Data Science and Management, 5(2), 57-65.

[13] Jin, Y. H., Oh, J., Choi, W., & Kim, M. K. (2022). Spatio-spectral decomposition of complex eigenmodes in subwavelength nanostructures through transmission matrix analysis. Nanophotonics, 11(9), 2149-2158.

[14] An, S., Zhu, H., Wei, D., Tsintotas, K. A., & Gasteratos, A. (2022). Fast and incremental loop closure detection with deep features and proximity graphs. Journal of Field Robotics, 39(4), 473-493.

[15] Zhou, J., Liu, L., Wei, W., & Fan, J. (2022). Network representation learning: from preprocessing, feature extraction to node embedding. ACM Computing Surveys (CSUR), 55(2), 1-35.

[16] Eltrass, A. S., Tayel, M. B., & Ammar, A. I. (2022). Automated ECG multi-class classification system based on combining deep learning features with HRV and ECG measures. Neural Computing and Applications, 34(11), 8755-8775.

[17] Yang, H., Li, L. L., Li, G. H., & Guan, Q. R. (2022). A novel feature extraction method for ship-radiated noise. Defence Technology, 18(4), 604-617.

[18] Zhou, Z., Dong, X., Li, Z., Yu, K., Ding, C., & Yang, Y. (2022). Spatio-temporal feature encoding for traffic accident detection in VANET environment. IEEE Transactions on Intelligent Transportation Systems, 23(10), 19772-19781.

[19] Xiong, Z., Mo, F., Zhao, X., Xu, F., Zhang, X., & Wu, Y. (2022). Dynamic texture classification based on 3D ICA-learned filters and fisher vector encoding in big data environment. Journal of Signal Processing Systems, 94(11), 1129-1143.

[20] Patro, K. K., Jaya Prakash, A., Jayamanmadha Rao, M., & Rajesh Kumar, P. (2022). An efficient optimized feature selection with machine learning approach for ECG biometric recognition. IETE Journal of Research, 68(4), 2743-2754.

Edited by: Bradha Madhavan
Special issue on: High-performance Computing Algorithms for Material Sciences
Received: Jan 17, 2024
Accepted: Mar 26, 2024